Tutorial on the Impact of the Synchronous Generator Model on Protection Studies

Normann Fischer, Gabriel Benmouyal, and Satish Samineni
Schweitzer Engineering Laboratories, Inc.

Tutorial on the Impact of the Synchronous Generator Model on Protection Studies

Normann Fischer, Gabriel Benmouyal, and Satish Samineni, *Schweitzer Engineering Laboratories, Inc.*

Abstract—The classical theory of representation of power swings in the impedance plane is based on the representation of synchronous generators as constant voltage sources. The classical model of a synchronous generator represents the machine as a constant voltage source behind the transient reactance in the direct axis. The classical model of synchronous generators is based on the assumption that the rotor flux linkage will not change during a short period of time following a major disturbance. In reality, with constant excitation voltage, the rotor flux linkage will decrease and the internal generator voltage will decrease accordingly. The addition of an automatic voltage regulator (AVR) boosts the excitation voltage following a disturbance so that the rotor flux linkage will be sustained and the generator internal voltage will be prevented from collapsing. The purpose of this paper is to show how power swing representation in the impedance plane will depart from the classical theory when complex AVRs are used on modern generators.

I. BASIC SYNCHRONOUS GENERATOR PHYSICAL PRINCIPLES

This paper is not intended to be an exhaustive review of synchronous generator physical and engineering principles, but rather an overview of fundamental and essential facts. It is assumed here that the reader is familiar with the two-axis model representation of synchronous machines [1].
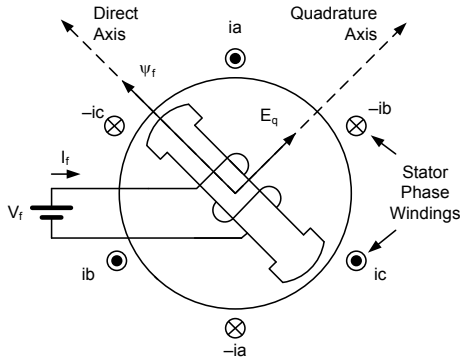

Fig. 1.   Synchronous generator basic mechanical and electrical structure

Fig. 1 represents a two-pole synchronous generator. The rotor winding is supplied with a dc exciter voltage V_f. A dc current I_f flows in the rotor winding to create a flux ψ_f in the generator direct axis. When the primary mover drives the generator and the generator rotates at synchronous speed, the flux will induce a voltage in the three-phase stator windings. When the generator is unloaded, we can measure an excitation or generator internal voltage at the terminals. This internal voltage, E_q in Fig. 1, is proportional to the current I_f and lies in the quadrature axis 90 degrees ψ_f. E_q is given by (1).

$$E_q = \omega M_f I_f \qquad (1)$$

In steady state, the current flowing in the rotor winding is equal to the exciter voltage divided by the winding resistance:

$$I_f = \frac{V_f}{r_f} \qquad (2)$$

The field winding has a self-inductance L_{ff}. A fundamental characteristic of a synchronous generator is the direct-axis open-circuit transient time constant T'_{d0}, the ratio of the field self inductance over its dc resistance:

$$T'_{d0} = \frac{L_{ff}}{r_f} \qquad (3)$$

The order of magnitude of this time constant, which is typically a few seconds, indicates that the voltage at the synchronous generator terminals cannot be changed instantaneously; in other words, the current in the field winding varies according to the field open-circuit time constant.

When the generator is loaded, the three-phase currents will create a flux, represented in Fig. 2 as $\psi_{ia+ib+ic}$. This flux is known as the armature reaction. The vectorial addition of the field flux and the armature reaction is the air-gap flux, which is represented as ψ_{ag}.
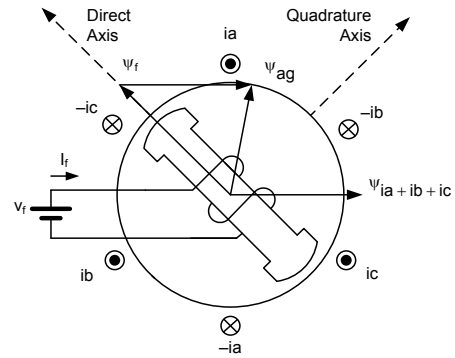

Fig. 2.   Armature reaction

The projection of the air-gap flux on the direct and quadrature axis, as in Fig. 3, defines the fluxes in the direct and quadrature axes as ψ_d and ψ_q.

The fluxes in the direct and quadrature axes create the corresponding voltages v_d and v_a along the same axes. We can demonstrate [1] these voltages with:

$$v_d = r_a i_d + \frac{d\psi_d}{dt} - \omega \psi_q \qquad (4)$$

and

$$v_q = r_a i_q + \frac{d\psi_q}{dt} + \omega\psi_d \qquad (5)$$

Fig. 3.   Fluxes in the direct and quadrature axis

A. The Synchronous Generator in the Steady State

In steady state, we can express the voltage phasor at the generator terminals in terms of the phasors in the direct and quadrature axes as follows:

$$V_t = V_d + jV_q \qquad (6)$$

In the same fashion, we can express the current phasor after it has been projected on the two axes as follows:

$$I_t = I_d + jI_q \qquad (7)$$

In steady state, (8) provides the vectors' relation linking the excitation voltage to the terminal voltage and current for a salient-pole machine.

$$E_q = V_t + r_a I_t + jx_d I_d + jx_q I_q \qquad (8)$$

Fig. 4 shows the corresponding generator vector diagram. In this figure, δ is the internal angle between the excitation voltage and the generator terminal voltage. In the same figure, φ is the angle between the generator terminal voltage and current that determines the power factor.
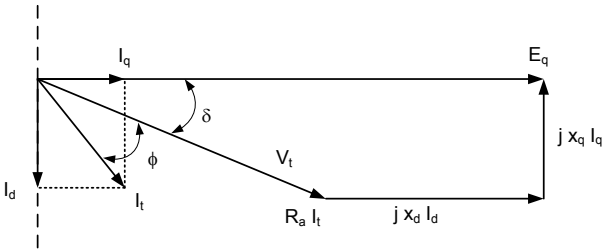

Fig. 4.   Salient-pole generator vector diagram in steady state

B. The Synchronous Generator in the Transient State

Based on the relations between the different vectors in the steady state as in Fig. 4, the fundamental theorem of the flux linkage provides some insight about the behavior of a generator in transient state. The theorem of flux linkage states that "the flux linkage of any closed circuit of finite resistance and finite e.m.f. cannot change instantly" [1]. In reality, the flux linkage will vary according to the circuit time constants. Applying this principle to a synchronous generator, one could state that the field flux does not change during a disturbance

or, if it changes, it will change slowly because of the long time constant associated with the rotor.

Consider the exciter voltage we obtain from (9):

$$E' = v_f = R_f i_f + \frac{d\psi_f}{dt} \qquad (9)$$

A new exciter voltage referred to the armature is defined in (10):

$$E_{ex} = \frac{\omega M_f E'_{ex}}{R_f} \qquad (10)$$

This new exciter voltage will have a value of 1 pu when the generator is open circuited and its terminal voltage is 1 pu. If we assume that the field flux does not vary following a disturbance, we can define a new fictitious voltage proportional to ψ_f that also does not vary in (11) [1]:

$$E'_q = \frac{\omega M_f}{L_{ff}}\psi_f \qquad (11)$$

We can then relate the new fictitious voltage to the excitation voltage with (12) [1]:

$$E'_q = E_q - (x_d - x'_d)i_d \qquad (12)$$

Fig. 5 shows a salient pole generator vector diagram in transient state by indicating the relation between E_q and E'_q.

In the transient state and following a disturbance, if we assume that the internal voltage E'_q remains constant, we can show the next relation between the internal voltage E'_q and the generator terminal voltage V_t with (13):

$$E'_q = V_t + jX'_d I_d + jX'_q I_q \qquad (13)$$

If we assume that the saliency is removed, in other words, $X'_d = X'_q$, we can define a new constant voltage internal E'_i that is equal to (14):

$$E'_i = V_t + jX'_d I_t \qquad (14)$$

This last voltage can represent a generator as a constant voltage source behind transient reactance, as in Fig. 6. We can therefore represent a generator as a constant voltage source behind the transient impedance if the following assumptions are in effect:

- The rotor flux linkage remains constant.
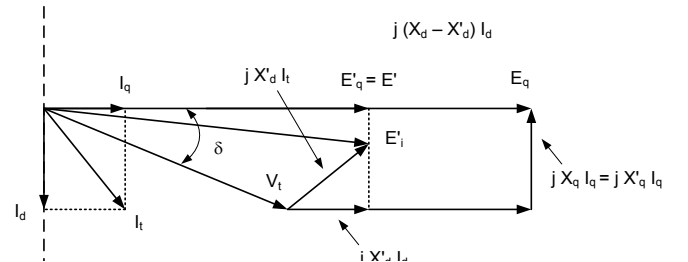- Saliency is removed. In other words, there exists only one reactance that is X'_d.

Fig. 5.   Salient-pole generator vector diagram in transient state
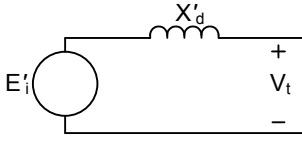
Fig. 6.   Representation of a synchronous generator as a constant voltage source behind transient reactance

If we assume that E'_q is not constant, a relation exists that provides the rate of change of this fictitious voltage with (15) [1]:

$$\frac{dE'_q}{dt} = \frac{E_{ex} - E_q}{T'_{d0}} \qquad (15)$$

When we do not assume a constant flux linkage following a disturbance, the rate of change of the voltage proportional to the rotor flux linkage is as in (15): a function of the exciter voltage E_{ex}, the excitation voltage E_q, and the generator rotor open circuit transient time constant T'_{d0}. Note that as the rotor time constant T'_{d0} increases, the rate of change of E'_q decreases.

To illustrate the impact of exciter voltage E_{ex} on E_q and E'_q following a disturbance close to the generator, consider the example of an unloaded generator, with unit terminal voltage, subjected to a three-phase short circuit at its terminals. The generator impedances are as in (16):

$$X_d = 1.15, X'_d = 0.37, X_q = X'_q = 0.75 \qquad (16)$$

Because the generator is unloaded, the identities in (17) are applicable prior to the short circuit:

$$V_t = E_{ex} = E_q = E'_q = 1.0$$
$$I_t = 0 \qquad (17)$$

If we follow the methodology indicated in [1], Fig. 7 shows the variation in time of the excitation voltage E_q when the short circuit is applied with different exciter voltages. At the moment the short circuit is applied, E_q will jump from 1.0 to 3.29 because of the fault current. E_q will then vary according to the exciter voltage applied. In manual mode ($E_{ex} = 1.0$), the excitation voltage will start dropping linearly. With a voltage regulator, as the exciter voltage jumps to its ceiling value (see Section II), the rate of change of the internal voltage drop decreases. The figure shows the variation of E_q with two regulator ceiling voltages: 2 and 3.5 pu. There exists a value for the exciter voltage (slightly smaller than 3.5 pu for the example) where the excitation system will sustain E_q. Above this value, E_q will increase linearly during the short circuit.

Fig. 8 uses the same example during the three-phase short circuit to illustrate the variation of E'_q. Following the application of the short circuit, E'_q does not change, because of the constant flux linkage principle. As for E_q, E'_q will drop linearly with low values of the exciter voltage E_{ex}. For E_q, there is a threshold value for E_{ex} where E'_q will remain unchanged during the short circuit. Above the threshold, E'_q will start increasing linearly rather than decreasing.

This example illustrates the impact of an autoregulator on generator internal voltage during a disturbance. An auto-regulator can increase the generator internal voltages during a disturbance. This capacity is directly related to improving the generator transient stability, as this paper explains later.
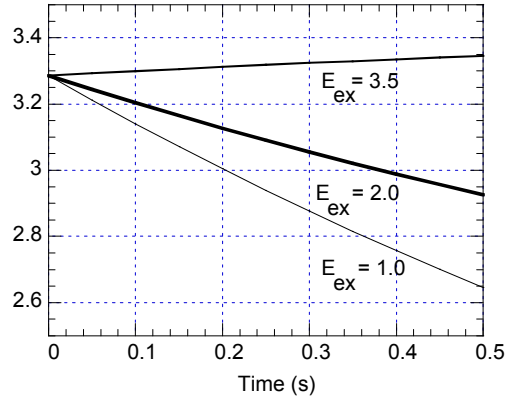

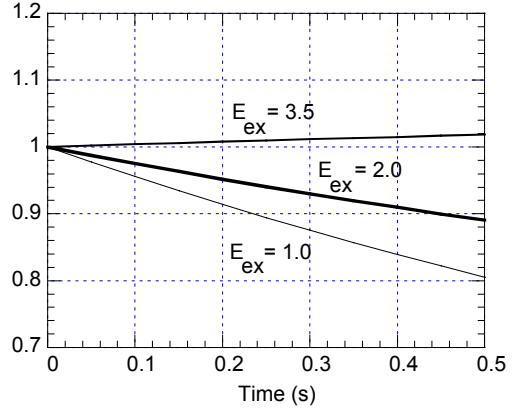Fig. 7. E_q variation with different excitation voltages E_{ex}

Fig. 8. E'_q variation with different excitation voltages E_{ex}

C. *The Notions of Synchronizing and Damping Torques*

Consider the simple network model of Fig. 9, where a generator represented as a constant voltage source behind the transient reactance supplies an infinite bus through an impedance Xe. This generator model is the classical model of a generator.
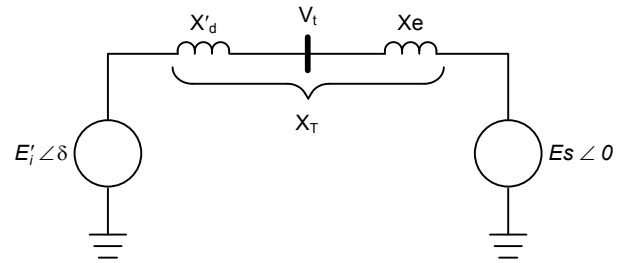

Fig. 9.   Elementary power network with classical representation of generator

We define the following:

ΔT_m is the variation of the mechanical power input to the generator in per unit (pu).

H is the inertia constant in seconds.

M is the inertia coefficient = 2H in seconds.

ω_0 is the base rotor electrical speed in radians per second (377 rad/s).

The control block diagram that Fig. 10 represents allows us to use the technique of small-signal analysis [2] [5] to study the dynamics of the elementary network in Fig. 9.

The total electrical torque that opposes the mechanical power input the synchronous machine produces is the sum of two synchronous and damping torques and is equal to (18):

$$\Delta T_e = \Delta T_{sync} + \Delta T_{damp} = K_1 \Delta\delta + K_D \Delta\omega \qquad (18)$$

The synchronous torque is proportional to the machine internal angle variation in (19):

$$\Delta T_{sync} = K_1 \Delta\delta \qquad (19)$$

The damping torque is proportional to the machine speed variation in (20):

$$\Delta T_{damp} = K_D \Delta\omega \qquad (20)$$

For the system in Fig. 9, we can demonstrate that K_1 is equal to (21) [2]:

$$K_1 = \left(\frac{E_i' E_s}{X_T}\right)\cos\delta_0 \qquad (21)$$

For the generator belonging to the network in Fig. 9 to be stable, both the synchronous and damping torques have to be positive. A lack of either of the two torques will render the generator unstable.
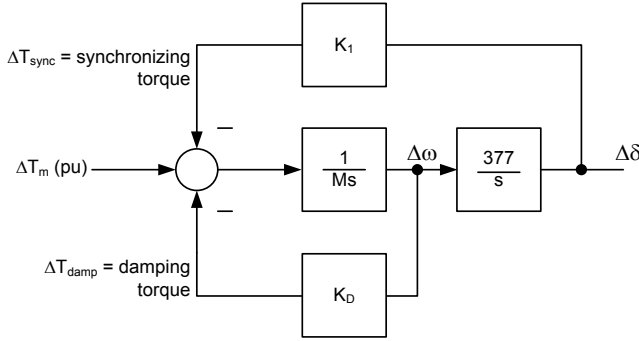

Fig. 10.   Control block diagram of an elementary power network

II. SYNCHRONOUS GENERATOR EXCITATION SYSTEMS

A. The Manual and Automatic Voltage Regulator (AVR)

The primary function of a synchronous generator excitation system is to regulate the voltage at the generator output. This paper focuses on present-day excitation static systems such as the one in Fig. 11.

In these systems, the input power for the static exciter is commonly derived from the machine terminals. A step-down transformer (excitation transformer PPT) feeds a three-phase controlled rectifier bridge that converts ac voltage into dc voltage. The dc output is connected to the machine field winding by brushes and collector rings.

In manual mode, either the level of the generator output voltage or the field current level (as in Fig. 11) is under the manual control of the operator. Although manual control of the excitation system still occurs on some old machines, organizations such as the North American Electric Reliability Corporation (NERC) recommend against this practice today because of the drawbacks and shortcomings that this mode of operation entails.

In automatic mode, a voltage set point is introduced in the summing point of the AVR. The excitation system compares this voltage set point to the generator output voltage measurement, and the comparison produces an error signal that adjusts the timing of the firing of the silicon-controlled rectifiers until the output voltage V_t equals the voltage set point. In steady state, the generator output voltage is therefore equal to the voltage set point.
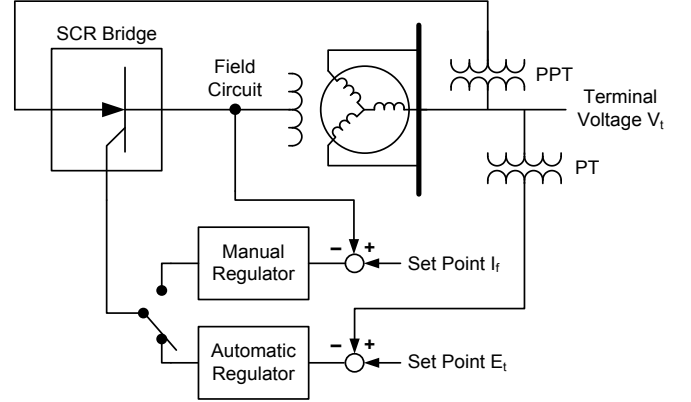

Fig. 11.   AVR principle with self-exciting generator

Fig. 12 represents the generic model of a static excitation as provided among others by [10]. Such models are intended as guidelines for stability studies. V_{ref} is the voltage setting, and V_C is the voltage measurement from the generator terminals. The difference between these two quantities constitutes the basic error signal. These models provide for additional error signals at the AVR summing point. V_S is the error signal from a power system stabilizer (PSS). V_{UEL} is the error signal from an under excitation limiter, which we describe later. In the excitation system of Fig. 12, an auction occurs between some signals; in other words, a high-voltage (HV) gate will pick out the input signal that has the highest level when a low-voltage (LV) gate picks out the signal that has the smaller one. This auctioneering action, when it occurs, allows some signals to take control of the AVR loop. As an example, following the AVR summing point, if the error signal from the UEL circuit is larger than the error signal from the summing point, the system gives priority to the UEL signal that takes control of the AVR loop. The output of the AVR is the voltage supplied to the field circuit. This voltage is bound and is of primary importance. The maximum voltage the excitation system supplies is commonly called the AVR ceiling. During a severe disturbance, such as a short circuit close to the generator terminals, the system will most likely apply this exciter ceiling voltage as the field voltage to counteract decreasing generator output voltage. Section I provides an example to demonstrate how the voltage regulator can sustain the generator internal voltage during a short circuit at the generator terminals.
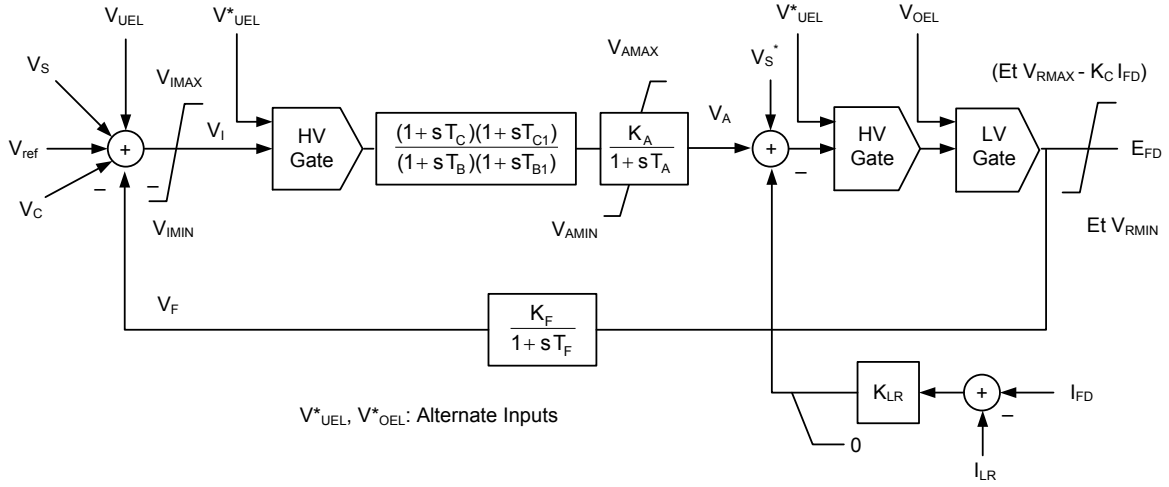
Fig. 12.   IEEE type ST1A excitation system

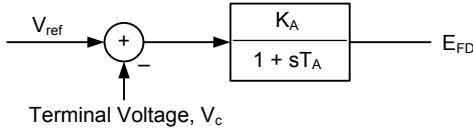Fig. 13 represents a simplified model of an AVR by a gain K_A, again, with a time constant.

Fig. 13.   Simplified representation of a static excitation system

B. The Power System Stabilizer

One negative effect of an AVR installed on a generator is that it decreases the internal damping torque when its gain K_A is increased (the synchronizing torque is, however, increased). Because of this, the regulator gain must be limited to some value between 15 and 25 in most situations [4], and this limitation then reduces the dynamic stability of the generator. Two solutions exist for this AVR gain limitation: 1) limit the AVR gain or 2) supplement the AVR with a PSS.

The PSS basic principle, as Fig. 15 shows, consists of measuring the change with respect to synchronous speed and sending a signal derived from this speed variation to the summing point of the AVR [2]. The net effect of the PSS action is to increase the generator damping torque in both steady and transient state. Another result of using the PSS is being able to increase the AVR gain K_A without affecting the overall generator stability.
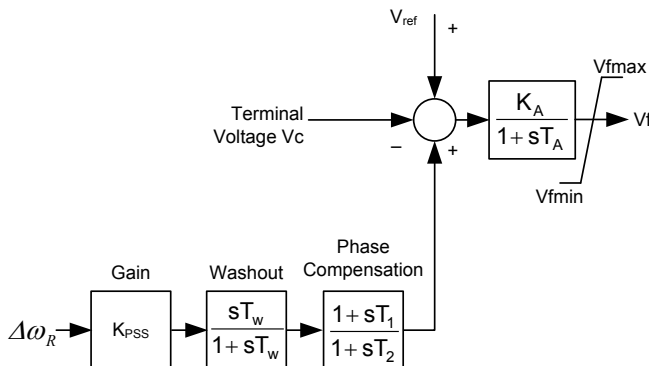
C. The Underexcitation Limiter

The purpose of an underexcitation limiter (UEL) is to prevent a generator from being operated in steady state in a determined underexcited region.

Consider the UEL model (type UEL2) in Fig. 15. This model comes from the recommended models in [11]. We can determine the UEL static or steady-state characteristic by setting the Laplacian operator "s" to zero and by looking at the condition when the error signal from the UEL circuit will be zero [1]. Equation (22) provides this condition:

$$P E_t^{-k1} KUP - E_t^{k2} KUV - Q E_t^{-k1} KUQ = 0 \qquad (22)$$

Expressing Q as a function of P, we obtain (23):

$$Q = P \frac{KUP}{KUQ} - E_t^{(k1+k2)} \frac{KUV}{KUQ} \qquad (23)$$

Equation (23) describes a straight line, as shown in Fig. 16, and represents the UEL characteristic in the P-Q plane. When the generator operating point falls below the line segment, the UEL produces a positive error that the system supplies to the AVR summing point. This positive error, in turn, has the effect of increasing the voltage setting or AVR voltage reference so that the generator terminal voltage increases until the generator operating point goes above the UEL limit straight-line characteristic [3] [5].
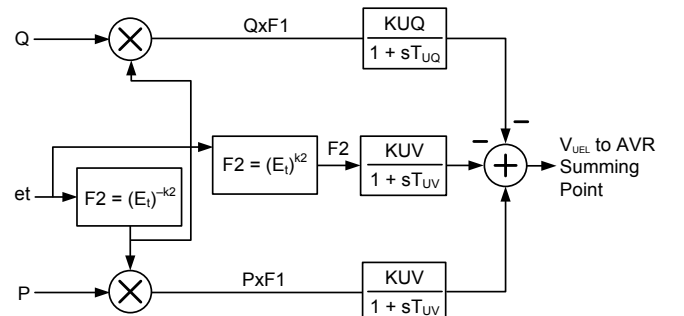

Fig. 15.   Example of a type UEL2 straight line UEL
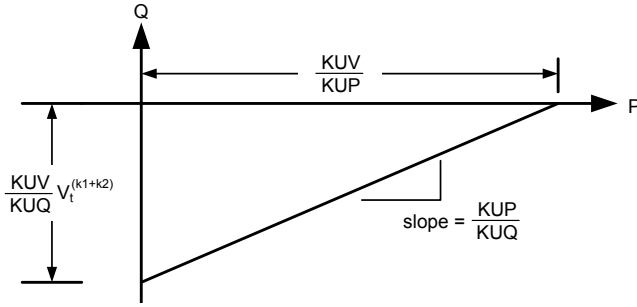

Fig. 14.   Principle of a PSS

Fig. 16.   Type UEL2 straight line characteristic

Reference [11] describes two additional UEL characteristics, one circular (type UEL1) and one multisegment straight line (type UEL3), that work on the same principles as type UEL2.

Keep in mind that, while the AVR and the PSS will improve the dynamic stability of a generator, the purpose of a UEL is to help prevent the generator from undergoing steady-state instability resulting from its operation in the underexcited region.

D. High-Speed, High-Ceiling Voltage Excitation Systems

A network disturbance resulting from a fault close to a generator reduces the generator's terminal voltage. If the generator excitation system is operated in manual mode, its internal voltage will decrease according to (15).

If the generator excitation system is under the control of an AVR, the voltage the AVR imposes on the field winding during the fault will depend upon the AVR speed, gain, and ceiling voltage. Consequently, the amount of boost that the generator internal voltage will receive depends upon these three factors.

It is generally recognized that a high-speed, high-gain, and high-ceiling AVR supplemented with a PSS is presently one of the best means to improve generator transient stability [2].

III. REVIEW OF CLASSICAL STEADY-STATE AND TRANSIENT STABILITY METHODS

A. Steady-State Stability

We can define the steady-state stability limit (SSSL) of a particular circuit of a power system as the maximum power at the receiving end of the circuit that we can transmit without loss of synchronism if we increase the load in very small steps and if we change the field currents after each increment so as to restore normal operating conditions [1].

Consider the elementary system of Fig. 17, which consists of a generator with constant internal voltage E_q that supplies an infinite bus through an impedance X_e. The conventional formula in (24) provides the steady-state power transfer equation for a salient-pole machine:

$$P = \frac{E_q\,E_s}{X_d + X_e}\sin\delta + E_s^2\,\frac{X_d - X_q}{2(X_d + X_e)(X_q + X_e)}\sin 2\delta \tag{24}$$

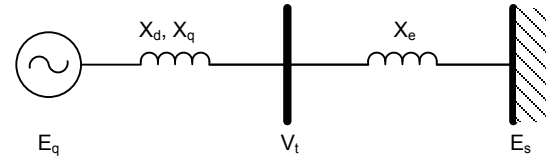In (24), δ is the angle between E_q and E_s, as in Fig. 18.

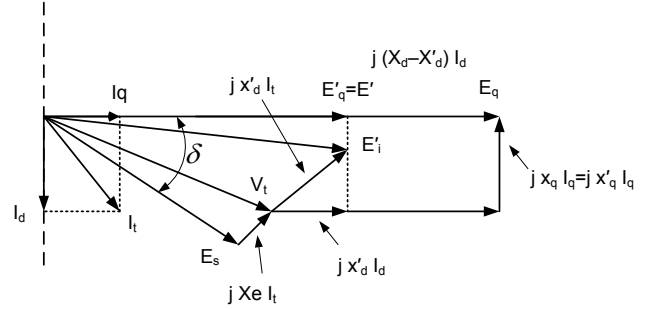Fig. 17.   Elementary generator system

Fig. 18.   Vector diagram of network in Fig. 17

Equation (24) allows us to determine the maximum power that we can transfer from the generator before reaching steady-state instability. We can also plot the stability limit in the P-Q plane. With manual operation, and if we assume that saliency has been removed, the classical SSSL is a circle with center and radius as in Fig. 19 [3] [5].

$$\text{Center} = j\frac{V_t^2}{2}\left(\frac{1}{X_e} - \frac{1}{X_d}\right)$$

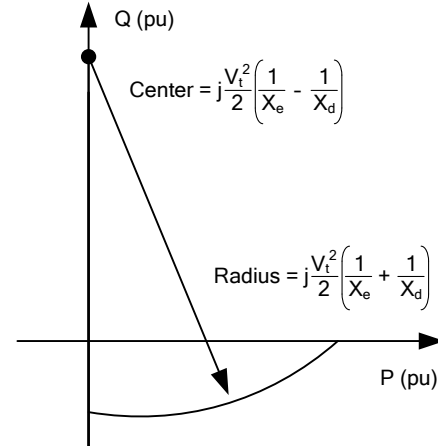$$\text{Radius} = j\frac{V_t^2}{2}\left(\frac{1}{X_e} + \frac{1}{X_d}\right)$$

Fig. 19.   SSSL with manual operation

Reference [5] introduced a technique that allows plotting of the SSSL when an AVR or an AVR-PSS combination is active in the system. Fig. 20 shows the various SSSLs (manual, AVR, and AVR-PSS) for a system corresponding to Fig. 17 with the characteristic values in Fig. 17. The following comments are worth mentioning:

- All three stability limits go through the point $-1/X_d$.
- The AVR stability limit expands the manual limit, provided the AVR gain is limited. Beyond a gain threshold, the SSSL with an AVR will infringe into the stability area of the manual case [5].
- The AVR-PSS combination allows an increased gain of the AVR to a higher value (100 in the example). The SSSL of the AVR-PSS combination goes much lower in the underexcitation region than the two other

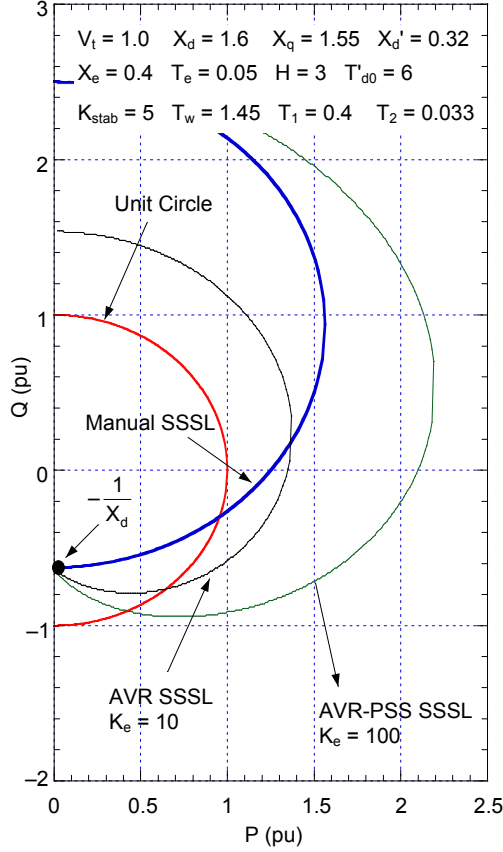limits (manual and AVR). The SSSL has, therefore, been substantially improved.

Fig. 20. Various SSSLs depending upon the nature of the exciter

B. Transient Stability

Transient stability is the ability of the power system to maintain synchronism when subjected to a severe transient disturbance such as a fault on a transmission line, loss of generation, or loss of a large load [2].

Modern techniques allow us to use such tools as transient stability programs or electromagnetic transients programs (EMTPs) to study power network transient stability. These two program types introduce extensive models of generators. Classical methods to study transient stability have used the equal-area criterion and have necessitated a power transfer equation in the transient state.

We can obtain a formula for the power transfer equation in transient stability by replacing E_q with E'_q and X_d with X'_d in (24):

$$P = \frac{E'_q E_s}{X'_d + X_e} \sin \delta + E_s^2 \frac{X'_d - X_q}{2(X'_d + X_e)(X_q + X_e)} \sin 2\delta \quad (25)$$

We can simplify the equation further by removing the saliency and replacing E'_q with E'_i so that we get:

$$P = \frac{E'_i E_s}{X'_d + X_e} \sin \delta \quad (26)$$

As an example, consider the case of a generator operated at unit terminal voltage and unit current with a power factor of 0.91. Equation (27) shows the generator impedances in pu values:

$$X_d = 1.15, X'_d = 0.37, x_q = X'_q = 0.75 \quad (27)$$

Equation (28) shows the external impedance:

$$X_e = 0.2 \quad (28)$$

For this condition of operation, we can compute the generator internal and infinite bus voltages in Fig. 18.

$$
\begin{aligned}
E_q &= 1.793 \\
E'_q &= 1.179 \\
|E'_i| &= 1.345 \\
|E_s| &= 0.935
\end{aligned}
\quad (29)
$$

Fig. 21 shows the three power transfer curves: one for the steady state and corresponding to (24) and two for the transient state corresponding to (25) and (26). In transient state, we can apply the equal-area criterion on the two transient state curves. One can see that the two curves in the transient state exhibit a much higher peak value, so we can expect a better transient stability if we were to use the curve in steady state.
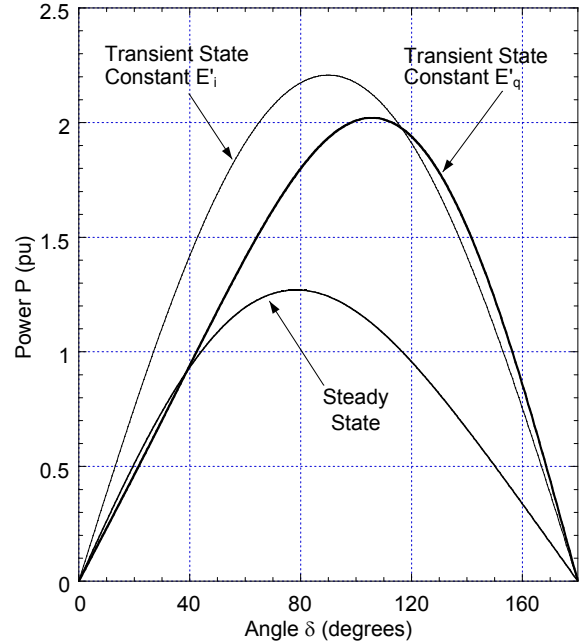

Fig. 21. Generator power angle curves in steady and transient states

IV. Classical Swing Impedance Characteristic

A. Classical Model of Generators

The classical swing impedance theory determines the impedance trajectory in the complex plane when the generator is represented as a constant voltage source, the angle of which varies with respect to an infinite bus (Fig. 22). This model of a generator is the same as the classical model shown in Fig. 9. In Fig. 22, we assumed that Xtr between the generator and the infinite bus represents the impedance of the step-up transformer and that Z_e corresponds to the series impedance of a transmission line.
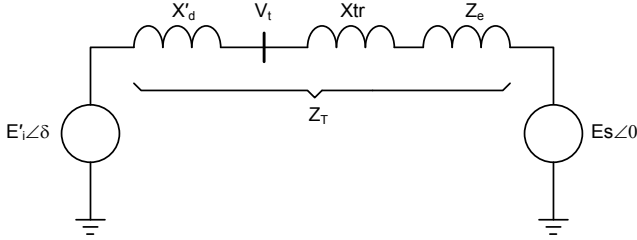

Fig. 22.   Generator classical model

B. Basic Theory of Swing Impedance

For the network model corresponding to Fig. 22, the classical theory of swing impedance allows us to determine the swing impedance characteristics in Fig. 23. The swing impedance characteristic depends primarily on the ratio n of the two source magnitudes:

$$n = \frac{E'_i}{E_s} \qquad (30)$$

When the two source magnitudes are equal ($n = 1$), the swing trajectory is a straight line perpendicular to the total impedance Z_T segment. The trajectory crosses the Z_T segment at its middle point when the phase angle δ between the two sources is 180 degrees. This point is called the swing center.

When ratio n is greater than one, the swing impedance is a circle in the upper part of the impedance plane. When n is smaller than one, the swing impedance trajectory will also be a circle, but it will be in the lower part of the impedance plane.

Fig. 24 shows a family of circles with different ratios n corresponding to the generator and network impedances in that figure.

As ratio n becomes increasingly greater or smaller than one, the circles become smaller.

C. Divergence From the Basic Theory

After a disturbance, the assumption that the generator is a constant voltage source is only valid for a short time, compared to T'_{d0}. In reality, the type and the characteristics of the excitation system in the generator determine the generator internal voltage and, therefore, ratio n.

With manual operation or constant voltage excitation, one might assume that the generator internal voltage will decrease after a disturbance. As a result, ratio n will become smaller than one; therefore, the impedance trajectory will follow circles in the lower part of the plane with radii that could eventually become smaller and smaller.

However, if the excitation system is an AVR, the excitation will sustain, and may boost, the generator internal voltage so that ratio n becomes greater than one. The change of the generator internal voltage depends upon the AVR characteristics: a slow-acting AVR could limit the rise of the internal voltage, but a fast-acting AVR could contribute to a rapid buildup of the internal voltage [3]. After the internal voltage builds up and ratio n becomes greater than one, the trajectory circles will move to the upper part of the impedance plane, with the circles decreasing as n increases (as shown in Fig. 24).
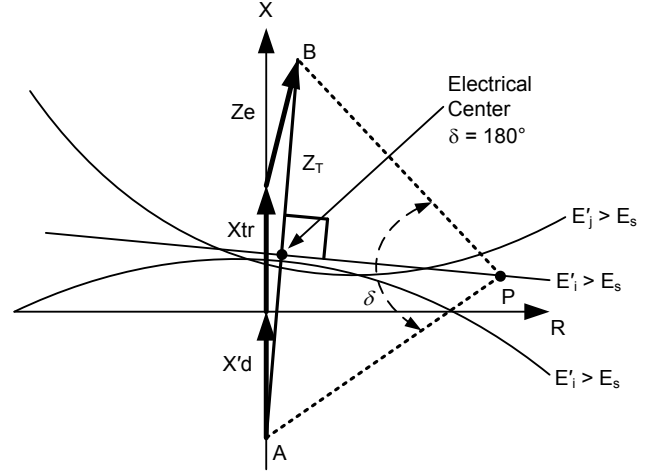

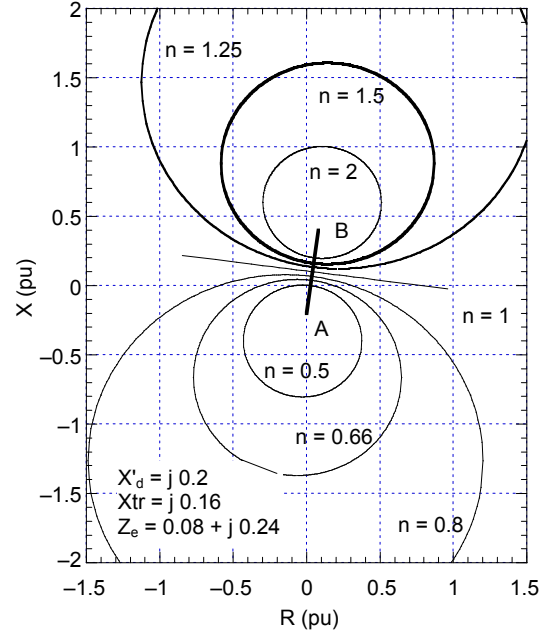Fig. 23.   Loss-of-synchronism characteristic in the impedance plane

Fig. 24.   Family of loss-of-synchronism impedance characteristics

V. Case Studies Using an EMTP

This section demonstrates how a generator responds after a disturbance when the generator excitation system is controlled in any of the following ways:

- Manually
- Via an AVR
- Via an AVR plus a PSS (AVR + PSS)

The generator used in the Real Time Digital Simulator (RTDS®) represents a set of 4 x 555 MVA generators (in the model, we consider them as a single 2220 MVA generator). Fig. 25 is a high-level representation of how the generator excitation system will be controlled in the RTDS.
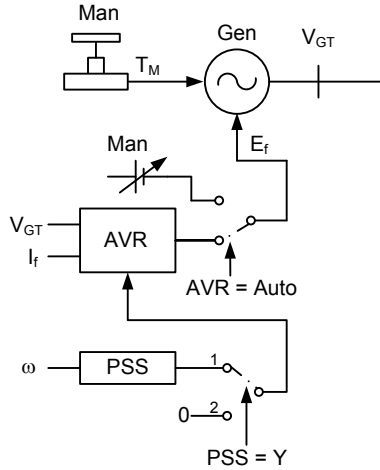

Fig. 25.   A high-level representation of the generator AVR and PSS controllers used in the case studies

We use a static excitation model as the AVR because of the rapid response of this type of excitation system. The model does not include a governor model because of the slow response of the governor compared to the exciter (AVR). The mechanical torque applied to the generator is kept constant (torque prefault = torque post-fault).

We obtained the power system used in this test from [2], Chapter 12, and show this system in Fig. 26.
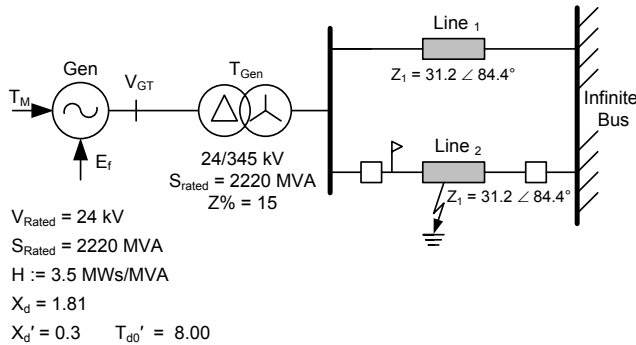

Fig. 26.   Representation of the model power system used for these case studies

We apply a three-phase fault to the system; after 85 ms, the fault is cleared. Switching the faulted line out of service clears the fault. The line is switched back into service after a predetermined dead time. Once the fault is cleared, the power system experiences a power swing. The aim of these simulations is to show how different excitation systems will affect the stability of the generator and that of the power system after a system disturbance.

A. Examples of Swings With Manual Excitation.

In the first case, the fault is cleared after 85 ms and the line reclosed after 500 ms. The system remains stable. Fig. 27 shows the voltages and currents as measured by a protection device in Line 2.
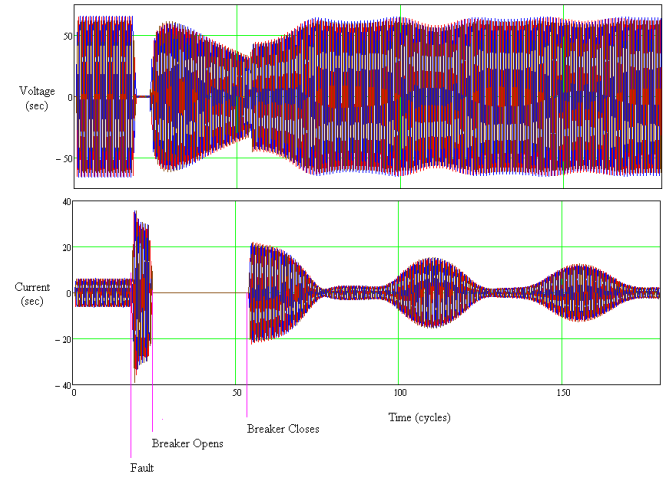

Fig. 27.   Voltage and current profiles for a three-phase fault with autoreclosing after 500 ms

The voltages and currents shown in Fig. 27 are the secondary voltages and currents; the CT and PT ratios are 400 and 3,000, respectively. By using the voltages and currents from Fig. 27, we can obtain the positive-sequence impedance and plot this in the impedance plane. Fig. 28 is a plot of the positive-sequence impedance after the breaker is closed (faulted line switched back into service).
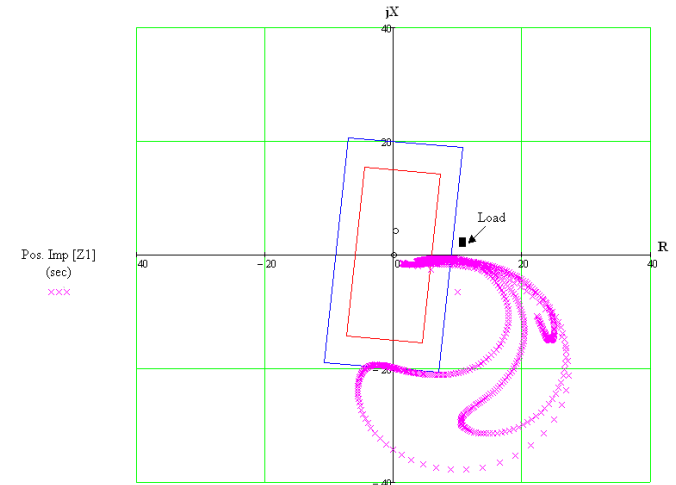

Fig. 28.   Positive-sequence impedance for the first case study

Using the data from Fig. 27, we can calculate the positive-sequence impedance magnitude. Fig. 29 is a plot of the positive-sequence magnitude. This plot shows how the positive-sequence impedance varies during a stable swing condition. The plot also shows that the rate of change of the impedance (dZ/dt) is not constant during a swing condition.
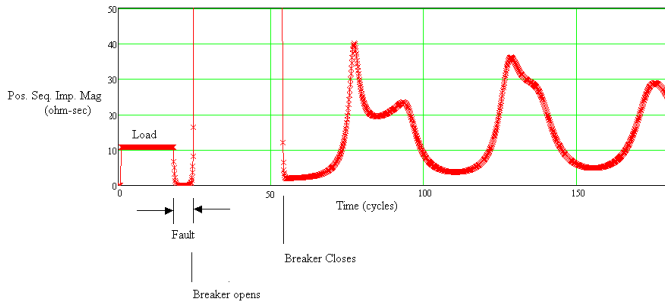
Fig. 29. Positive-sequence impedance magnitude for the manual excitation case where the generator maintains synchronism

Fig. 30 shows the generator speed, active power, and reactive power for this case.
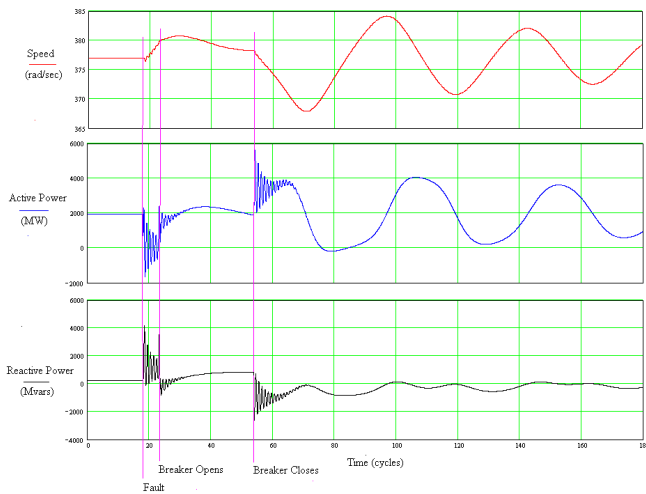

Fig. 30. Response of the generator speed, active power, and reactive power outputs before, during, and after the applied fault

Remember that there are two power lines in this system, so even with one line out of service the generator is still connected to the power system and can export power. We confirm this by examining the current in the second line (Line 2 in Fig. 31).
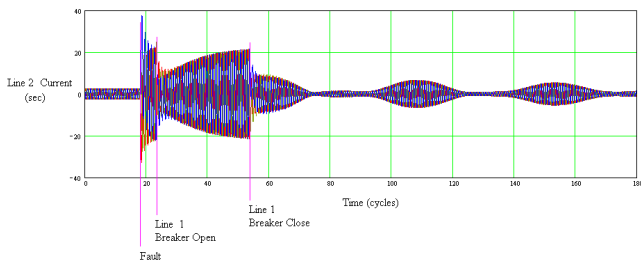

Fig. 31. A plot of the current in the adjacent unfaulted line before, during, and after the fault

The current, and subsequently the power, through the second line increases. The reason for this increase is twofold:

- When the fault is cleared, the system experiences a power swing because the kinetic energy stored in the rotor increases the rotor speed.
- The generator is being supplied with its predisturbance mechanical power of 1,960 MW.

The machine wants to export its stored mechanical energy as well as the input mechanical energy. The effect of this is that the current through the unfaulted, in-service line increases. This affects the generator terminal voltage because increasing current through the line results in decreasing terminal voltage. The terminal voltage decreases because of the increase in the internal voltage drop ($jX_{d'}I_t$) of the generator. Because the excitation voltage is fixed, E_x = constant, the generator EMF E_q does not increase. As a result, the terminal voltage V_t decreases, which means that the machine cannot export its input and stored energy unless the current increases. For this case of manual excitation, the generator has enough synchronizing torques available to remain in synchronism with the system when the faulted line is returned to service after a dead time of 500 ms.

In the second case of the manual excitation mode, we apply the same fault; the fault is again cleared after 85 ms, but the line is reclosed (returned to service) after one second. This time, however, the system (generator) does not experience a stable swing but becomes unstable. Fig. 32 is a plot of the voltages and currents a protective device would see for this instance.
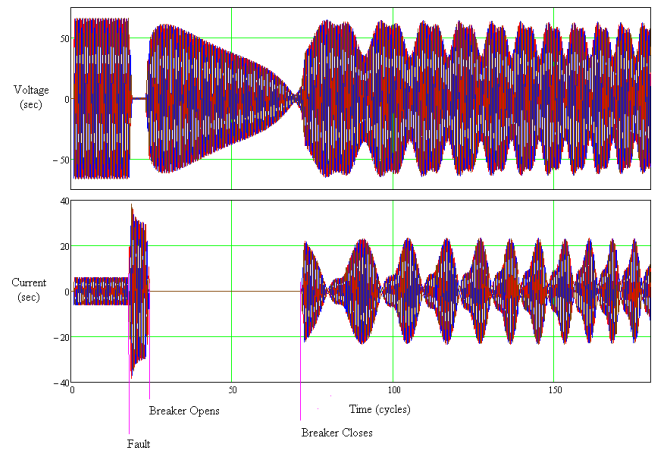

Fig. 32. The voltage and current profile for the three-phase fault whereby the faulted line is reclosed after 1 second (unstable swing case)

If we use the data from Fig. 31, calculate the positive-sequence impedance, and plot this impedance in the impedance plane, we get the curves we would expect from the theory. Fig. 33 demonstrates use of this theory.
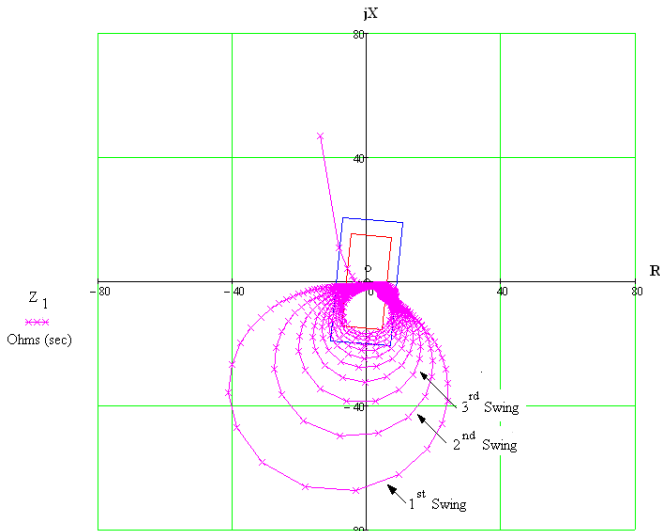
Fig. 33. A plot of the positive-sequence impedance, in the impedance plane, derived from the voltage and current signal in Fig. 32

Also notice that in Fig. 32, as the terminal voltage decreases, $jX_{d'}I_d$ increases and the value of n decreases, which means that the diameter of the swing circle decreases for each consecutive swing. Note that when Line 1 reclosed (see Fig. 32), the machine voltage was lower than the system voltage (infinite bus) or, stated another way, $n < 1.0$. Therefore, the power swing is in the lower-left-hand side of the impedance plane. This agrees with the theory presented.
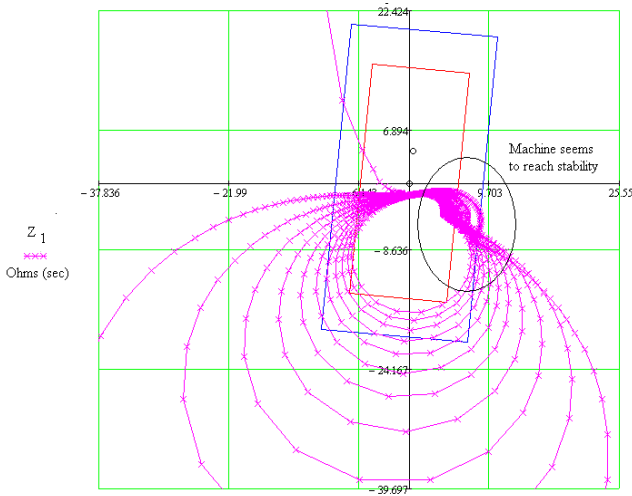

Fig. 34. An enlarged plot of the positive sequence impedance

Close examination of Fig. 33 reveals an anomaly in the curves; they are not perfect, concentric circles, but seem to have a flat spot. Based on the voltage and current graphs of Fig. 32, it appears that the machine may become stable after the breaker has closed and the pole has slipped. For approximately three cycles, both lines carry nominal current and the terminal voltage seems stable. However, after three cycles, the voltage collapses and the machine becomes unstable.

Fig. 35 shows the variation in the positive-sequence impedance for the different swings. After the pole slip, the system seems to stabilize when the impedance stabilizes. This agrees with what we observed in Fig. 34.
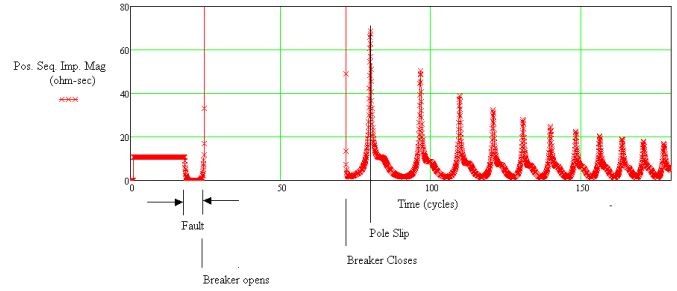

Fig. 35. A plot of the positive-sequence impedance magnitude for the case when the generator becomes unstable

Examining the generator speed, active power, and reactive power, as in Fig. 35, one can see that the generator becomes unstable (has zero synchronizing torque) before the circuit breaker closes. This instability occurs because the huge drop in interval voltage inside the generator leaves the voltage at the terminal V_t so low that the generator cannot export power. Therefore, the generator electrical output does not match the mechanical input power. The imbalance between the mechanical power and electrical power causes energy to be stored in the rotor in the form of kinetic energy, resulting in rotor acceleration. This is one of the major drawbacks of a manually controlled exciter: it cannot boost excitation voltage after the fault is cleared. If the generator internal voltage E_i can increase, thereby reducing the internal voltage drop, the terminal voltage V_t increases because the internal voltage drop ($jX_{d'}I_t$) decreases as a result of the reduced current.

For this case, the critical reclosing time of Line 1 is 600 ms, or 36 cycles. At this time, the machine synchronizing torque equals zero. We can see that the machine speed begins to increase and continues increasing, even when the breaker is reclosed. In practice, overspeed, overcurrent, or pole-slip protection would have probably tripped the generator/ machine.
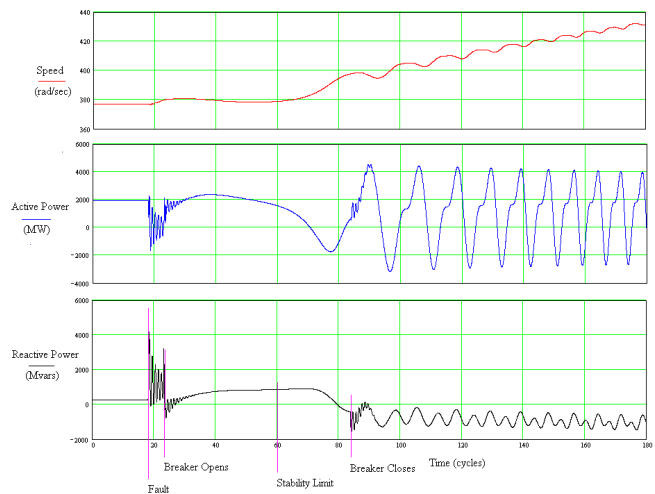

Fig. 36. Plot of the generator speed, active power, and reactive power when the generator experiences an unstable power swing

Another factor to consider when using manual excitation on a generator is the reclosing time of critical lines. As shown in the second case, manual excitation can lead to the generator becoming unstable after a system disturbance.

B. Examples of Swings With AVR Enabled

For this case study, the AVR is enabled and we subject the system to the same fault and reclosing time that caused the manually excited system to become unstable. This study will help demonstrate the effect of the AVR.

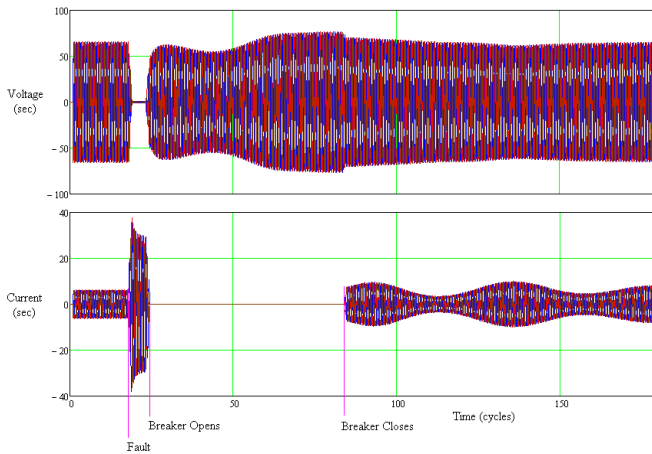Fig. 37 is a plot of the voltage and current waveforms for the protected line.

Fig. 37. A plot of the voltage and current with the AVR enabled for the case that caused instability in the manually excited generator

From the voltage and current plot, we can see that the system experiences a stable power swing after the line is reclosed. What is different about the plot in Fig. 37 compared to the plots in Fig. 27 and Fig. 32 is that the voltage in Fig. 37 does not begin to collapse when the fault is cleared. This has a very important effect because the terminal voltage stays high, even though the voltage drop ($jX_{d'}I_t$) in the machine is approximately the same as in the manually excited case. This means the machine can export the same amount of electrical power as it receives in mechanical input power. Therefore, no uncontrolled acceleration occurs. Terminal voltage maintains its prefault value because the AVR boosts the generator internal voltage. Using the data from Fig. 37, we can calculate the positive-sequence impedance after the line comes back into service. This is the impedance such as a distance relay protecting the line would see.

Fig. 38 is a plot of the positive-sequence impedance in the impedance plane. The plot has a time frame of approximately 100 cycles (1.67 seconds) and begins when the breaker recloses. After approximately 15 seconds, the positive-sequence impedance reaches its value, which is identical to its prefault value, indicated as "Load" in Fig. 38.
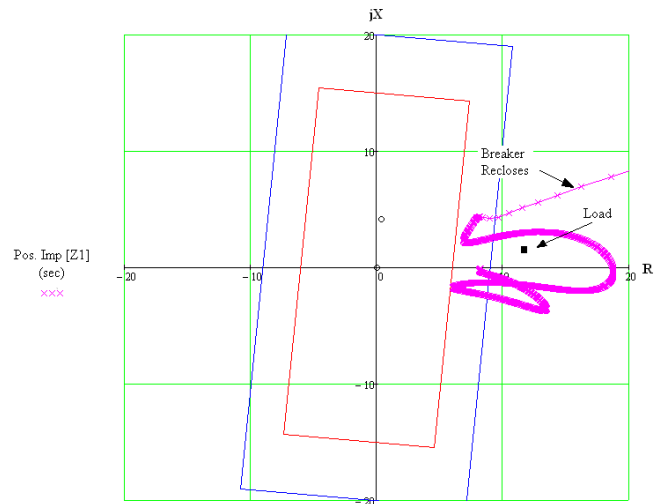

Fig. 38. A plot of the positive-sequence impedance in the impedance plane for the case where the AVR is enabled

The impedance plot in Fig. 38 is further proof that the swing is stable. Note, however, that the trajectory of this plot is not as smooth as that of the manual excitation case in Fig. 28. Instead, this trajectory has discontinuity in its derivative because the AVR tries to keep the terminal voltage within defined limits. When the AVR tries to maintain the voltage within these limits, it regulates the reactive power the generator exports or imports. This is reflected in the impedance plane in terms of the reactive component (X). This anomaly is not visible in the positive-sequence impedance magnitude plot in Fig. 39, because Fig. 39 reflects the magnitude changes caused by the active power decreasing (R is increasing), while the reactive power remains almost constant (X remains constant).
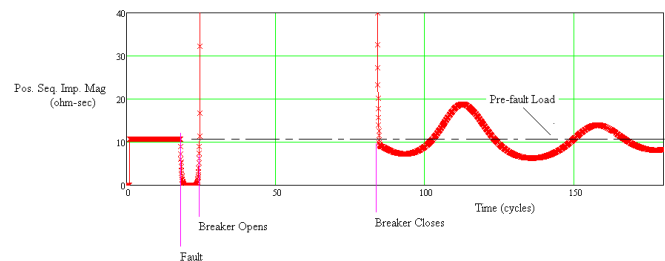

Fig. 39. A plot of the positive-sequence magnitude for the case where the AVR is enabled

Fig. 40 is the response of the generator for the applied conditions. Initially, the speed, active power, and reactive power are at a constant level (prefault condition). During the fault, the machine speed increases. This is to be expected because the amount of electrical active power the generator exports is not the same as the amount of mechanical power it imports. Also, during the fault the active power export decreases and the reactive power export increases, which agrees with the theory. Once the fault clears, the machine speed begins to stabilize and the machine begins to export more active power (MWs) than it did during the prefault condition. This is because the machine has stored up kinetic energy in the rotor during the fault, energy that is now also being exported to the power system. Because the machine is exporting more electrical power than it is receiving mechanical power, the rotor speed begins to decrease as the generator uses up the stored kinetic energy. Up to this point (±27 cycles after fault clearance [450 ms]), the machine behaves almost identically for the manually excited and the automatically excited case. Moving forward, however, differences begin to appear. In the manually excited case, the generator active power export begins to decrease, which results in increasing speed. This downward spiral continues until the machine slips a pole and becomes unstable. The instability occurs because the increased voltage drop inside the generator collapses the terminal voltage, preventing the generator from exporting the electrical active power that it is receiving in the form of mechanical energy. When the AVR is enabled, it keeps the terminal voltage at a more or less constant level after the fault is cleared.
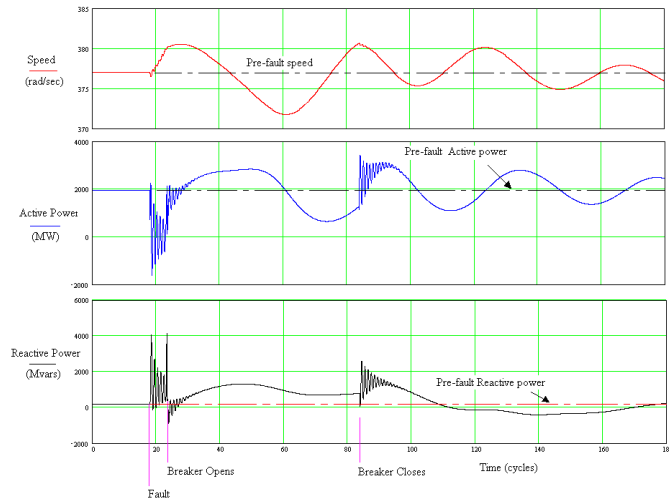

Fig. 40.   A plot of the generator speed, active power, and reactive power for the case where the AVR is enabled

From Fig. 40, we can see that the generator does not settle back to its prefault condition rapidly after the fault is cleared. As mentioned before, the generator achieves its prefault state after about 15 seconds.

Fig. 41 shows the response of the AVR. The three-phase fault on the line reduces the terminal voltage to near zero during this fault, and the AVR tries to compensate for the low terminal voltage by boosting the generator internal voltage (E_i). During the fault, the AVR reaches the voltage maximum limit (see Fig. 12).
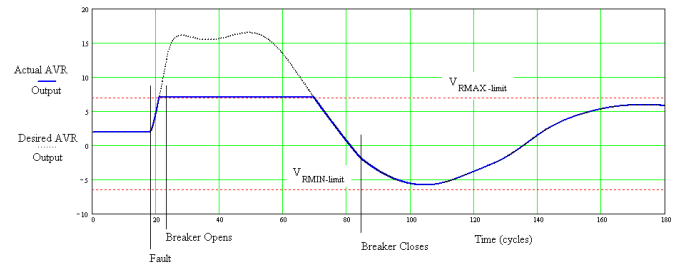

Fig. 41.   Output of the AVR

This boost in internal voltage helps maintain generator stability during the time the faulted line breaker is open, allowing the generator to export the same amount of active power as the amount of mechanical power it imports. As mentioned before, the current the generator exports for the first 27 cycles after the fault is cleared is almost similar for both cases (see Fig. 42), but after this point, the manually excited generator current continues to increase because the machine is trying to export real power. So, even though reactive power is linked to voltage, voltage is necessary to export active power from a generator. Thus, the boost in internal voltage resulting from the AVR gives the generator the synchronizing torque to maintain synchronism with the system.
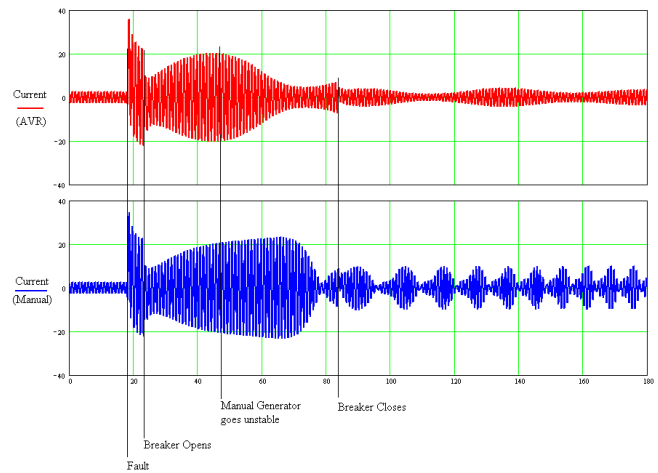

Fig. 42.   A comparison of the line current in the unfaulted lines for the case with and without the AVR enabled

C. Examples of Swings With AVR and PSS Enabled

For this third and final case, both the AVR and the PSS will be enabled, and we will subject the system to the same condition as previously mentioned. Fig. 43 is a voltage and current plot for the applied fault and the reclose.
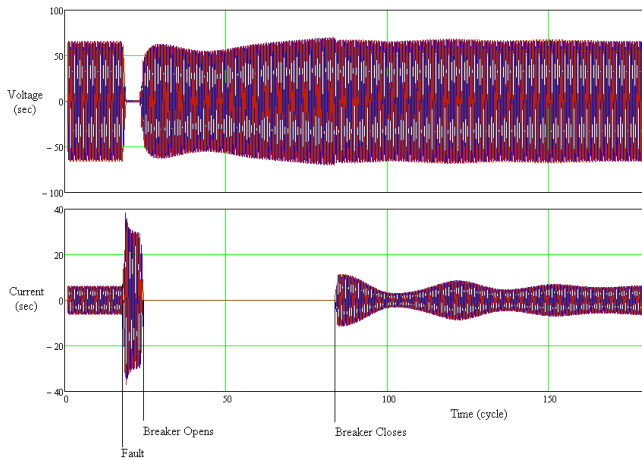

Fig. 43.   A plot of the voltage and current with the AVR and PSS in service

The voltage and current plot shows that the generator remains stable during the open interval time and when the breaker recloses. If we now plot the positive-sequence impedance (see Fig. 43 and Fig. 44), we see that the swing is more damped and the impedance does not traverse a large section of the impedance plane, as was the case when only the AVR was enabled.
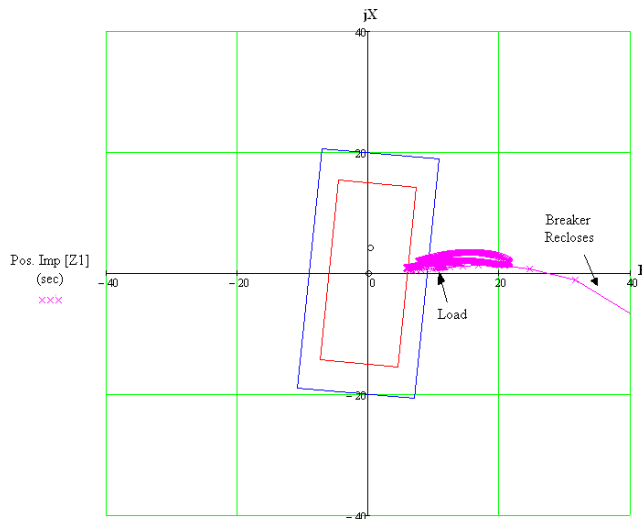

Fig. 44.   A plot of the positive-sequence impedance in the impedance plane for the case where the AVR and PSS are enabled

If we enlarge Fig. 44, we see that the impedance variation after each swing decreases more (see Fig. 45) than for the case with only the AVR. The plot in Fig. 45 occurs over the same time frame, 3 seconds or 180 cycles, as the one in Fig. 38. From this plot, we can clearly see the effect of the PSS. The PSS results in the impedance returning more rapidly to its prefault state.
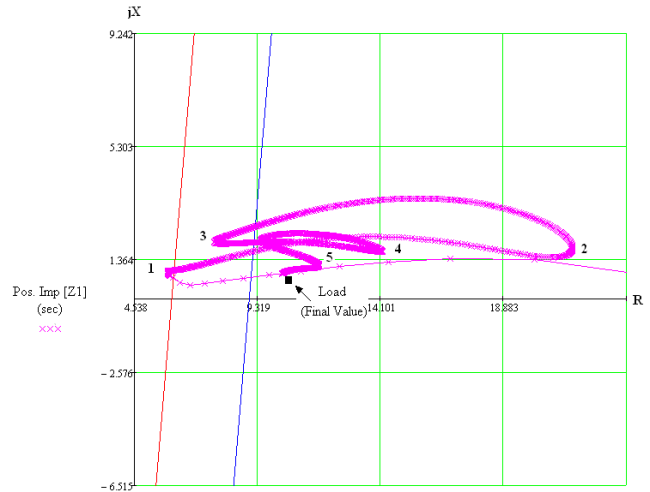
Fig. 45.   Enlarged plot of Fig. 44 to better show the trajectory of the positive-sequence impedance after the line is reclosed

If we examine the positive-sequence magnitude plot (see Fig. 46), we see that the rate of change of impedance $|dZ|/dt$, is initially as large (for the first swing) as for the plot without the PSS. However, we can see that this is no longer the case for subsequent swings, and these oscillations are damped out more rapidly than in the plot without the PSS. Therefore, we can see that the PSS damps out the oscillations.

Fig. 46.   A plot of the positive-sequence impedance magnitude for the case where AVR and PSS are enabled

If we now examine the generator speed, active power, and reactive power (Fig. 47), we can see that the machine returns to its prefault value more rapidly with the PSS also enabled than for the same case with only the AVR enabled.

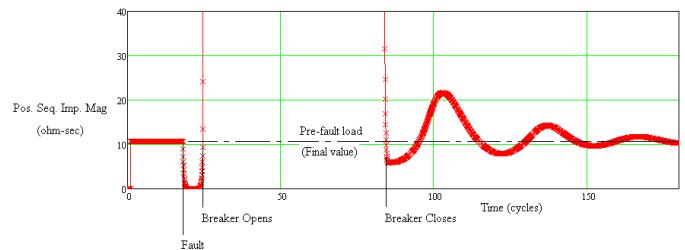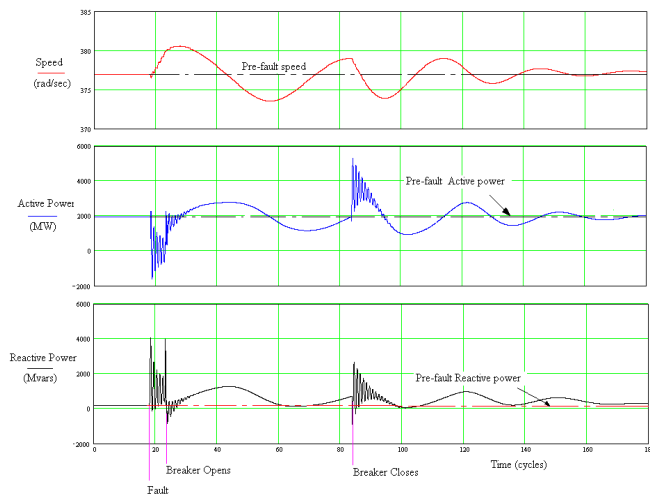Fig. 47. A plot of the machine speed, active power, and reactive power when the AVR and PSS are both enabled

Fig. 48 shows the output of the PSS and the AVR for the above condition. At fault inception, the machine initially loses speed and then gains speed. This initial drop in speed results in the PSS issuing a negative gain in the excitation. After this initial decrease in speed, the machine speed increases and the PSS and AVR both drive the AVR to its upper limit. It is interesting that the PSS causes the AVR to be driven to the upper and lower limits more often than when only the AVR is enabled. This occurs because the PSS wants to drive the change in speed of the machine to zero.
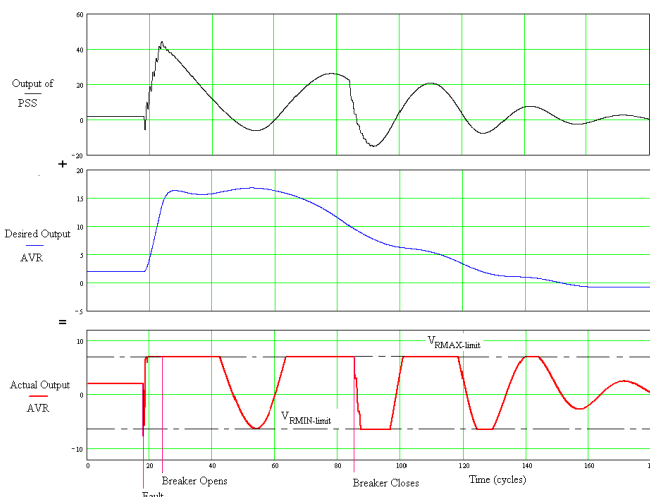

Fig. 48. A plot of the signals that are input and output from the AVR for the case with the AVR and PSS enabled

Note that the PSS can damp out the change in speed by regulating the power the machine exports. This is because the PSS can control the generator terminal voltage, and the machine power is regulated so that the oscillation of the machine cancels out (absorbs) the power system oscillations.

VI. CONCLUSIONS

1. For short-circuit studies, where only the fault current magnitude is of concern, we can use a constant voltage source instead of a complete generator model, reducing the complexity of the system model.

2. Generators with manual excitation experience a decrease of the generator internal voltage (E_i) following a system disturbance, such as a fault, close to the generator terminals. This decrease in internal voltage significantly reduces the generator's synchronizing ability after the disturbance.

3. An AVR significantly improves generator steady-state stability, provided that the gain of the AVR is limited and that the AVR is not operating at its limits before the disturbance. The AVR boosts the generator internal voltage during a system disturbance; this boost increases the generator synchronizing torque, allowing the generator to return to synchronism after the disturbance.

4. An AVR will help increase the synchronizing torque of a generator but will reduce the damping torque. Because of this, the AVR gain will have to be limited in most cases.

5. A PSS increases the damping torque of a generator and allows increasing the AVR gain without compromising the generator's dynamic stability. A PSS therefore improves the dynamic stability of the generator more than an AVR alone.

6. In transient stability studies, generators modeled with constant excitation will constitute the worst-case scenario with respect to system stability following a disturbance. AVRs and PSSs in the generators should substantially improve system stability.

VII. APPENDIX A: NOMENCLATURE

The nomenclature used for generator mathematical model symbols corresponds to the convention of [1].

E_q: excitation voltage or steady-state internal voltage
E'_q: quadrature component of transient internal voltage
E'_{ex}: exciter voltage
E_{ex}: exciter voltage referred to the armature
I_d: direct-axis component of the output current
I_q: quadrature-axis component of the output current
L_{ff}: field circuit self-inductance
R_f: field circuit resistance
M_f: mutual inductance between the field and any armature phase
r_a: armature phase resistance
T'_{d0}: direct-axis transient open-circuit time constant
T'_d: direct-axis transient short-circuit time constant
V_d: direct-axis component of the terminal voltage
V_q: quadrature-axis component of the terminal voltage
X_d: direct-axis synchronous reactance
X_q: quadrature-axis synchronous reactance
X'_d: direct-axis transient reactance
ψ_f: field circuit flux linkage
ψ_d: direct-axis component of the air-gap flux
ψ_q: quadrature-axis component of the air-gap flux
ω: generator speed in rad per second

VIII. APPENDIX B

In general, the per unit system is well understood; the apparatus MVA rating is used as the base MVA and the nominal voltage is used as the base voltage. From these, then, we can calculate the base impedance and currents.

For a generator, the situation is more complicated in that we have a field winding (excitation winding on the rotor) and an armature winding (on the stator). The field winding is excited from an excitation system/circuit. The excitation system has a per unit value based on the field current required to produce one per unit voltage on the stator along the air-gap line. The generator per unit system is based on its apparent power rating (MVA) and its nominal rating (kV) [base2]. However, we need to match the exciter with the generator, and this leads to a dilemma: what per unit system do we use when modeling a generator system?

We find that the generator has two per unit systems:

- Reciprocal per unit system: Used for modeling the generator armature (main machine) and the system, based on the generator MVA rating and nominal terminal voltage.
- Nonreciprocal per unit system: Used to model the generator excitation system. One per unit exciter voltage (field voltage) is equal to one per unit armature voltage (terminal voltage) along the air-gap line.
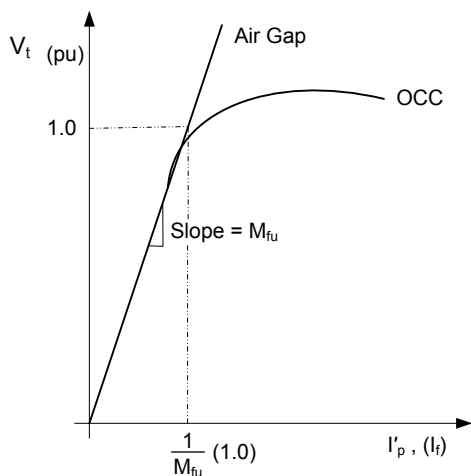

Fig. 49.   Synchronous machine open circuit characteristic

Let us determine a relationship between the current and voltage in nonreciprocal and reciprocal per unit systems. To do this, let us examine an unloaded (open circuited) generator, where $i_d = i_q = 0$.

We know the following:

$$e_d := -\psi_q = L_q \bullet i_q = 0 \qquad (iq = 0)$$

$$e_q := \psi_d = L_d \bullet i_d + M_f \cdot i_f = M_f \cdot i_d \qquad (id = 0)$$

If we now look at Fig. 49, we see that the field current needed to produce one per unit of terminal voltage (E_t) on the air-gap line is given by:

$$V_t := e_q = \omega \bullet M_{fu} \bullet I'_p = 1.0 \text{ pu}$$

but $\omega = 1$, so

$$e_q = M_{fu} \bullet I'_p$$

For the reciprocal per unit system, we can calculate the field current, I'_p, required to generate the rated stator voltage as follows:

$$I'_f := \frac{1}{M_{fu}} (\text{pu})$$

This generates the corresponding field current:

$$E_{ex'} = R_f \bullet I'_p = \frac{R_f}{M_{fu}}$$

By definition, we know that corresponding exciter output current I_f is 1.0 pu.

Therefore, $I_f := M_{fu} \bullet I'_f$ with a corresponding exciter voltage output:

$$E_f := \frac{M_{fu}}{R_f} \bullet E_{ex'}$$

Remember that, physically, the exciter output voltage and current are the same as the generator-field current and voltage. The exciter is connected via slip rings to the generator's field winding. We only make the distinction in the per unit system to allow the independent selection of a per unit system, thus allowing for modeling of the generator excitation system and the main generator. Fig. 50 is a simple sketch illustrating how to convert from the reciprocal per unit system to the non-reciprocal per unit system and vice versa.
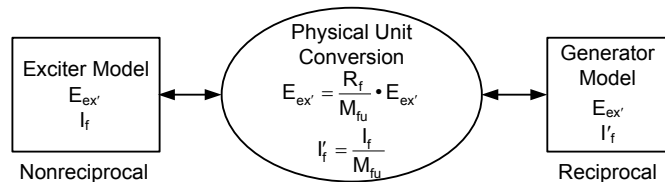
Fig. 50.   Per unit conversion between excitation system and synchronous machine

However, to refer physical units (actual values) from one system to the other, we have to use a different approach. We know the following:

$$E_q := \omega \bullet M_f \bullet I_f \text{ and } I_f = \frac{E_f}{R_f}$$

$$E_q := \omega \bullet \frac{M_f}{R_f} \bullet E_f \text{ and let } \gamma = \omega \frac{M_f}{R_f}$$

We can now relate E_f to E_q via γ, which is similar to relating the voltage of one winding of a transformer to that of another winding:

$$\left(E_1 = \frac{n_1}{n_2} \bullet E_2 \right)$$

The following sketch illustrates how to move from the non-reciprocal system to the reciprocal system and vice versa.

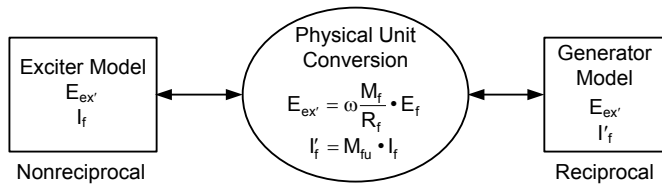Fig. 51. Physical unit conversion between excitation system and synchronous machine

A. Transient State Analysis

Let us now examine the excitation circuit when the generator is subjected to a system transient such as a power system fault or a switching operation:

$$E_{ex'} = R_f \bullet I'_f + \frac{d\psi_f}{dt} \quad \text{(nonreciprocal base)} \tag{31}$$

$$E_{ex'} = \omega \frac{M_f}{R_f} \bullet E_{ex'} \quad \text{(reciprocal base)} \tag{32}$$

$$\varpi \frac{M_f}{R_f} \bullet E_{ex'} = \omega \frac{M_f}{R_f} \bullet R_f \bullet I'_f + \omega \frac{M_f}{R_f} \bullet \frac{d\psi_f}{dt} \tag{33}$$

[converting (31) to a reciprocal base]

We know the following:

$$E_q = \omega \bullet M_f \bullet I'_f \tag{34}$$

$$T_{do'} = \frac{L_{ff}}{R_f} \tag{35}$$

During a fast change of armature current (fast compared to transient decrement, but not faster than the subtransient decrement), the flux linkage, ψ_{fd}, of the field remains substantially constant (i.e., $d\psi_{fd}/dt \approx 0$). This nearly constant flux linkage results in a new fictitious internal armature voltage proportional to the field flux linkage:

$$E_{q'} = \omega \bullet \frac{M_f}{L_{ff}} \bullet \psi_f \tag{36}$$

When we substitute (35) and (36) into Part C of (33), we get the following:

$$\omega \bullet \frac{M_f \bullet \psi_f}{R_f} = \frac{L_{ff}}{R_f} \bullet \omega \bullet \frac{M_f}{L_{ff}} \bullet \psi_f = T_{do'} \bullet E_{q'}$$

Substituting (32) into Part A and (34) into Part B of (33), we obtain the following:

$$E_{ex'} = E_q + T_{do}' \bullet \frac{E_{q'}}{dt}$$

$$\frac{E_{q'}}{dt} = \frac{E_{ex'} - E_q}{T_{do'}} \tag{37}$$

Now let us revisit some generator flux equations:

$$\psi_d = M_f \bullet I'_f - L_d \bullet i_d \tag{38a}$$

$$\psi_q = -L_q \bullet i_q \tag{38b}$$

$$\psi_f = L_{ff} \bullet I'_f - \frac{3}{2} \bullet M_f \bullet i_d \tag{38c}$$

Let us examine the difference between the quadrature axis voltages, E_q and E_q:

$$E_q - E_{q'} = \omega \bullet M_f \bullet I'_f - \omega \bullet \frac{M_f}{L_{ff}} \bullet \psi_f$$

[using (34) and (36)]

$$\tag{39}$$

If we substitute (38c) into (39), we get the following:

$$E_q - E_{q'} = \omega \bullet M_f \bullet I'_f - \frac{\omega \bullet M_f}{L_{ff}} \bullet \left(L_{ff} \bullet I'_f - \frac{3}{2} \bullet M_f \bullet i_d \right)$$

$$= \omega \bullet M_f \bullet I'_f - \frac{\omega \bullet M_f}{L_{ff}} \bullet L_{ff} \bullet I'_f + \frac{3}{2} \bullet \frac{\omega \bullet M_f^2}{L_{ff}} \bullet i_d$$

$$= \frac{3}{2} \bullet \frac{\omega \bullet M_f^2}{L_{ff}} \bullet i_d \tag{40}$$

If we know that the field is closed but not energized ($\psi_f = 0$), and we apply this to (38c), we get the following:

$$I'_f = \frac{3}{2} \frac{M_f}{L_{ff}} \bullet i_d \tag{41}$$

Substituting (41) into (38a), we get the following:

$$\psi_d = M_f \bullet \frac{3}{2} \bullet \frac{M_f}{L_{ff}} \bullet id - L_d \bullet i_d$$

$$\frac{\psi_d}{-i_d} = L_d - \frac{3}{2} \bullet \frac{M_f^2}{L_{ff}}$$

$$= L_d' \text{ (for a generator, for a motor, } \psi_d = L_d \bullet i_d)$$

$$\frac{3}{2} \bullet \frac{M_f^2}{L_{ff}} = L_d - L_d' \tag{42}$$

Substituting (42) into (40), we get the following:

$$E_q - E_{q'} = \omega \bullet (L_d - L_d') \bullet i_d$$

$$E_q - E_{q'} = (x_d - x_d') \bullet i_d \tag{43}$$

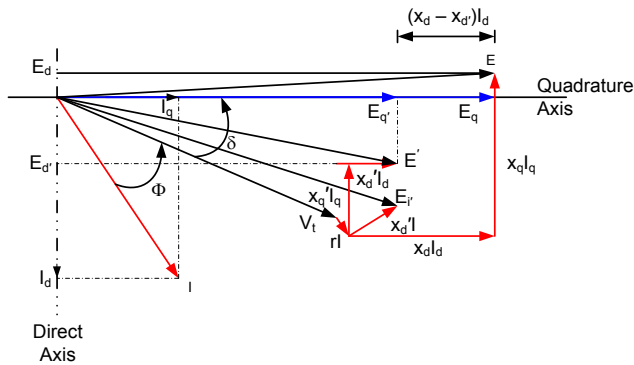If we now wrap all of this into a phasor diagram, we get the following:

Fig. 52. Phasor diagram of a synchronous machine during the transient state

IX. References

[1] E. W. Kimbark, *Power System Stability: Synchronous Machines*, Dover Publications, Inc., New York.

[2] P. Kundur, *Power System Stability and Control*, New York: McGraw-Hill, 1994.

[3] G. Benmouyal, "The Impact of Synchronous Generators Excitation Supply on Protection and Relays," proceedings of the 34th Annual Western Protective Relay Conference, Spokane, WA, October 2007.

[4] IEEE Standard 421.5-1992, *IEEE Recommended Practice for Excitation System Models for Power System Stability Studies*, 1992.

[5] F. P. DeMello and C. Concordia, "Concepts of Synchronous Machine Stability as Affected by Excitation Control," IEEE Transactions on Energy Conversion, Vol. PAS−88, No. 4, pp. 316−329, April 1969.

[6] IEEE Task Force on Excitation Limiters, "Underexcitation Limiter Model for Power System Stability Studies," IEEE Transactions on Energy Conversion, Vol. 10, No. 3, September 1995.

[7] D. Reimert, *Protective Relaying for Power Generation Systems*, Boca Raton: CRC Press, 2006.

[8] IEEE Power Engineering Society, *IEEE Tutorial on the Protection of Synchronous Generators*, 95 TP 102.

[9] IEEE Standard C37.102/D7−200X, *Guide for AC Generator Protection*, April 2006.

[10] ANSI Standard C50.13-1989, Requirements for Cylindrical Rotor Synchronous Generators, 1989.

[11] ANSI Standard C50.12-1982, Standard for Requirements for Salient-Pole Synchronous Generators and Generator/Motors for Hydraulic Turbine Applications, 1982.

[12] R. Sandoval, A. Guzmán, and H. J. Altuve, "Dynamic Simulations Help Improve Generator Protection," proceedings of the 33rd Annual Western Protective Relay Conference, Spokane, WA, October 2006.

X. Biography

Normann Fischer received a Higher Diploma in Technology, with honors, from Witwatersrand Technikon, Johannesburg in 1988, a B.S.E.E., with honors, from the University of Cape Town in 1993, and an M.S.E.E. from the University of Idaho in 2005. He joined Eskom as a protection technician in 1984 and was a senior design engineer in Eskom's Protection Design Department for three years. He then joined IST Energy as a senior design engineer in 1996. In 1999, he joined Schweitzer Engineering Laboratories, Inc. as a power engineer in the Research and Development Division. He was a registered professional engineer in South Africa and a member of the South Africa Institute of Electrical Engineers.

Gabriel Benmouyal, P.E. received his B.A.S. in Electrical Engineering and his M.A.S. in Control Engineering from Ecole Polytechnique, Université de Montréal, Canada, in 1968 and 1970, respectively. In 1969, he joined Hydro-Québec as an Instrumentation and Control Specialist. He worked on different projects in the field of substation control systems and dispatching centers. In 1978, he joined IREQ, where his main field of activity was the application of microprocessors and digital techniques for substation and generating-station control and protection systems. In 1997, he joined Schweitzer Engineering Laboratories, Inc. in the position of Principal Research Engineer. He is a registered professional engineer in the Province of Québec, an IEEE Senior Member, and he has served on the Power System Relaying Committee since May 1989. He holds over six patents and is the author or coauthor of several papers in the field of signal processing and power networks protection and control.

Satish Samineni received his B.E. degree in electrical and electronics engineering from Andhra University College of Engineering, Visakhapatnam, India. He received his Master's degree in Electrical Engineering from the University of Idaho in 2003. Since 2003, he has been with Schweitzer Engineering Laboratories, Inc. in Pullman, Washington, where he presently is a Lead Power Engineer. His research interests include power electronics and drives, power system protection, synchrophasor-based control applications, and power system stability.